

1 **The Importance of Adsorption for CCN Activity and**  
2 **Hygroscopic Properties of Mineral Dust Aerosol**

3

4 **Prashant Kumar<sup>1</sup>, Athanasios Nenes<sup>1,2</sup>, and Irina N. Sokolik<sup>2</sup>**

5 <sup>1</sup>School of Chemical & Biomolecular Engineering, Georgia Institute of Technology,  
6 Atlanta, GA, 30332, USA

7 <sup>2</sup>School of Earth & Atmospheric Sciences, Georgia Institute of Technology, Atlanta, GA,  
8 30332, USA

9 Correspondence to: A. Nenes ([athanasios.nenes@gatech.edu](mailto:athanasios.nenes@gatech.edu))

10 **Abstract**

11 This study uses published data on dust-water interactions to examine the importance  
12 of including water adsorption effects when describing the hygroscopic and cloud  
13 condensation nuclei (CCN) behavior of mineral dust aerosol. Adsorption activation  
14 theory (AT) better represents fresh dust-water interactions than Köhler theory (KT), as *i*)  
15 a consistent set of adsorption parameters can describe the hygroscopic behavior of dust  
16 (under both sub and supersaturated conditions), *ii*) the dependence of critical  
17 supersaturation,  $s_c$ , with particle dry diameter,  $D_{dry}$ , is closer to observations. The long  
18 adsorption timescale could also contribute to the large differences observed between dry  
19 and wet generated dust hygroscopicity. If KT and AT are consistently applied to the same  
20 dust size distribution, KT predicts up to tenfold higher CCN and 40% higher droplet  
21 number concentration than AT. This profoundly different behavior between the theories  
22 suggests that both may be required for a comprehensive description of atmospheric dust  
23 CCN activity.

## 24 **1. Introduction**

25 Mineral dust is ubiquitous in the atmosphere and represents a dominant type of  
26 particulate matter by mass. Dust particles can act as cloud condensation nuclei (CCN),  
27 giant CCN (GCCN) (e.g., Rosenfeld et al., 2001; Levin and Cotton, 2008), or ice nuclei  
28 (IN) (e.g., DeMott et al., 2003; Field et al., 2006) affecting cloud microphysics, albedo,  
29 and lifetime. Despite its well-recognized importance, assessments of dust impacts on  
30 clouds and climate are highly uncertain. In this study, we address the role of dust as CCN  
31 with the goal to provide an improved representation of dust CCN activation in the climate  
32 models.

33 Dust CCN activity is currently described by Köhler theory (herein KT; Köhler,  
34 1936), which is based solely on the contribution of the solute and curvature effects upon  
35 water equilibrium vapor pressure. KT implies that dust particles devoid of any solute  
36 would require very high ambient supersaturations (dictated by the Kelvin equation) to act  
37 as CCN. It is well known however that adsorption of water on insoluble particles  
38 (especially clays) can lead to hygroscopic growth similar to deliquescent salts (e.g.,  
39 Schuttlefield et al., 2007). Past studies have demonstrated that calcite ( $\text{CaCO}_3$ ) (a mineral  
40 with very low solubility compared to deliquescent salts) and Arizona Test Dust (ATD)  
41 can interact with water vapor and adsorb multiple layers of water under subsaturated  
42 conditions (Gustafsson et al., 2005; Vlasenko et al., 2005; Hatch et al., 2008). This  
43 interaction implies that dust mixtures and individual minerals with hydrophilic insoluble  
44 surfaces can affect water activity of aerosol (especially when the solute fraction of  
45 particles is low) with largely ignored implications for predicted CCN activity. Henson  
46 (2007) and Sorjamaa and Laaksonen (2007) recognized this gap, and developed

47 adsorption activation theory (AT) to describe the activation of hydrophilic insoluble  
48 CCN. The Sorjamaa and Laaksonen (2007) formulation is based on the FHH (Frenkel,  
49 Halsey and Hill) adsorption model (and constrained by two adjustable parameters,  $A_{FHH}$ ,  
50  $B_{FHH}$ ). Kumar et al. (2009) incorporated FHH-AT into a droplet activation  
51 parameterization for use in regional and global models, assuming that the aerosol  
52 constitutes an external mixture of “soluble” (KT) and “insoluble” (AT) particles.

53 Even if constrained by the same CCN activity or hygroscopic growth data, predicted  
54 CCN concentration and cloud droplet number,  $N_d$ , can differ between using KT and  
55 FHH-AT because: *i*) the relationship between particle critical supersaturation,  $s_c$ , and dry  
56 diameter,  $D_{dry}$ , differs between theories, resulting in a different predicted CCN spectrum  
57 even if the same size distribution is used, and, *ii*) KT particles require substantially more  
58 water to activate than FHH-AT particles with the same  $s_c$  (Kumar et al., 2009).  
59 Competition for water vapor in a cloud parcel during activation of KT particles can thus  
60 be more intense than for FHH-AT particles, leading to a different parcel maximum  
61 supersaturation,  $s_{max}$ , and droplet number.

62 In this study, we substantiate the importance of considering water vapor adsorption  
63 effects on the activation of mineral dust particles. This is done by fitting published CCN  
64 activity and hygroscopic growth data to the KT and FHH-AT, and examining whether  
65 each theory can *i*) describe subsaturated hygroscopic growth and CCN activity with one  
66 set of water-interaction parameters, and, *ii*) reproduce the observed dependence of  $s_c$  with  
67 respect to  $D_{dry}$ . Finally, we evaluate the differences in the CCN number and droplet  
68 number concentrations predicted by KT and FHH-AT, using the consistent parameters  
69 and the same aerosol size distribution.

## 70 **2. Comparison of Köhler and Adsorption Activation Theories**

71 KT provides a relationship between the equilibrium vapor pressure of an aqueous  
72 droplet as a function of its wet diameter and exhibits a maximum value termed as critical  
73 supersaturation,  $s_c$ , at a characteristic critical wet diameter,  $D_c$ . Particles exposed to  
74 ambient supersaturation above  $s_c$  typically activate into cloud droplets (Nenes et al.,  
75 2001). In KT,  $s_c$  depends on the amount of solute in the dry particle, which is related to  
76 its chemical composition and size. Petters and Kreidenweis (2007) parameterized the  
77 solute term of KT in terms of a hygroscopicity parameter,  $\kappa$ , which was derived from the  
78 relationship between  $D_{dry}$  and  $s_c$ .  $\kappa$  can be used to directly compare the hygroscopicity of  
79 aerosol over a wide range of composition, with  $\kappa \rightarrow 0$  for completely insoluble particles  
80 (for which  $s_c \sim D_{dry}^{-1}$ ) to  $\kappa \rightarrow 1.4$  for the most hygroscopic atmospheric aerosol (for which  
81  $s_c \sim D_{dry}^{-3/2}$ ). According to KT, a constant value of  $\kappa$  should be able to describe both  
82 aerosol subsaturated water uptake (where relative humidity, RH, is below 100%) and  
83 predict CCN activity (RH > 100%).

84 FHH-AT is similar to KT, except that the solute term is replaced with an adsorption  
85 term modeled by the FHH isotherm (Crittenden and Thomas, 1998). The adsorption  
86 parameter  $B_{FHH}$ , strongly affects the shape of the equilibrium curve, and largely  
87 determines the existence and value of  $s_c$  and  $D_c$  (Kumar et al., 2009). As with KT,  $s_c$  in  
88 FHH-AT can be related to  $D_{dry}$  as  $s_c = CD_{dry}^x$ . Particles with an appreciable soluble  
89 fraction follow KT, and  $x \sim -1.5$  when  $\kappa > 0.2$ . In FHH-AT,  $x$  varies between -0.8 and -1.5,  
90 depending on  $A_{FHH}$ ,  $B_{FHH}$  (Kumar et al., 2009).

91

### 92 3. Evidence for Adsorption Activation

93 Figure 1a shows published data (symbols) of  $s_c$  as a function of  $D_{dry}$  (Koehler et al.  
94 2009; Sullivan et al., 2009) for different dust types and individual mineral particles  
95 generated in the lab either with the use of a dry fluidized bed, or via wet atomization from  
96 an aqueous suspension of dust particles. The CCN activity data are fitted to a power law  
97 expression,  $s_c = CD_{dry}^x$ , from which the “experimental” exponent,  $x_{exp}$ , is determined  
98 (Table 1).  $A_{FHH}$  and  $B_{FHH}$  and the corresponding exponent,  $x_{FHH}$ , were determined from  
99 fitting the FHH-AT model (Figure 1a, lines) to the experimental data via least squares  
100 minimization. The KT fits to the data (expressed in terms of  $\kappa$ ) are given by Koehler et al.  
101 (2009) and Sullivan et al. (2009), from which the corresponding KT exponent,  $x_\kappa$ , is  
102 computed. The values of the exponents, adsorption parameters ( $A_{FHH}$ ,  $B_{FHH}$ ), and  $\kappa$   
103 (determined by Koehler et al., 2009, and Sullivan et al., 2009) are presented in Table 1.

104 In Figure 1b,  $x_\kappa$  (circles) and  $x_{FHH}$  (squares) are plotted against  $x_{exp}$  for all dust  
105 samples and individual minerals. With the exception of  $\text{CaCO}_3$  and  $\text{CaSO}_4$  (calcium  
106 sulphate) (where  $x_\kappa \rightarrow -1$  because of the very low  $\kappa$ ),  $x_\kappa \sim -1.5$ .  $\text{CaCO}_3$  (representing fresh  
107 unprocessed dust) and  $\text{CaSO}_4$ ,  $\text{CaC}_2\text{O}_4 \cdot \text{H}_2\text{O}$  (calcium oxalate monohydrate or COH)  
108 (representing atmospherically processed mineral dust) are better described by FHH-AT,  
109 as  $x_{FHH}$  is in perfect agreement with  $x_{exp}$ . For wet-generated ATD, Owens Lake (OL),  
110 Canary Island Dust (CID), and oxalic acid ( $\text{C}_2\text{O}_4\text{H}_2$ ),  $x_{FHH}$  lies closer than  $x_\kappa$  to the 1:1  
111 line.  $x_\kappa$  for dry Saharan Dust (SD), ATD and wet  $\text{Ca}(\text{NO}_3)_2$  are closer to  $x_{exp}$  than  $x_{FHH}$ ;  
112 this is expected for  $\text{Ca}(\text{NO}_3)_2$  because it is highly soluble (deliquescence  $\text{RH} = 49\%$ ;  
113 Fountoukis and Nenes, 2007), but not for dry ATD and SD. The large scatter ( $\text{R}^2 < 0.7$

114 for the  $s_c$ - $D_{dry}$  data for dry ATD) and potential size-dependant composition (for SD) may  
 115 explain this.

116 Another indication that KT may be an incomplete description of the dust CCN  
 117 activity presents itself in the value of wet-dust  $\kappa$  parameters, and the implications thereof.  
 118 If the aerosol can be considered as a mixture of a soluble salt with molar volume  
 119  $(M_s/\rho_s)$ , effective van't Hoff factor  $\nu_s$ , and volume fraction  $\varepsilon_s$ , then

120  $\kappa = \left(\frac{M_w}{\rho_w}\right)\left(\frac{\rho_s \nu_s}{M_s}\right)\varepsilon_s$ , where  $(M_w/\rho_w)$  is the molar volume of water. Assuming that the

121 hygroscopic fraction of dust behaves like ammonium sulfate gives  $\left(\frac{M_w}{\rho_w}\right)\left(\frac{\rho_s \nu_s}{M_s}\right) = 0.61$

122 (Petters and Kreidenweis, 2007). Therefore, the dust  $\kappa$  parameters can be used to infer an

123 “equivalent soluble volume fraction”, computed as  $\varepsilon_s = \frac{\kappa}{0.61}$ . If KT indeed applies, then

124  $\varepsilon_s$  should reflect the true soluble fraction of dust. From the values of  $\kappa$  reported in Table

125 1,  $\varepsilon_s = 0.58, 0.65$ - $1.78$ , and  $0.43$  for wet ATD, OL, and CID, respectively. Such a large

126 soluble fraction in fresh dust is much larger (or even impossible if larger than unity) than

127 the expected 2% soluble mass fraction in ATD (Vlasenko et al., 2005) and 3-37% in OL

128 (Koehler, 2008). Koehler et al. (2009) attribute this enhanced hygroscopicity to

129 redistribution of the soluble material among the insoluble dust cores, particularly in the

130 smaller size range. Given that KT implies  $s_c \sim \varepsilon_s^{-0.5} D_{dry}^{-1.5}$ ,  $\varepsilon_s$  will have to scale with  $D_{dry}^{0.3}$

131 for KT to yield  $x_\kappa = x_{exp} \sim -1.36$ . This means that  $\varepsilon_s$  varies more than 60% over the

132 diameter range (40 – 200nm) reported in the Koehler et al. (2009) experiments, so that

133 the soluble fraction at the high  $s_c$  should be close to unity. This is certainly possible; the

134 hygroscopicity parameter, however, does not seem to change considerably when subsets  
135 of the activation data (especially in the higher supersaturation range) are separately  
136 considered. This implies that KT may not completely describe the CCN activity of dust,  
137 so that other processes, such as physisorption, could contribute to the water activity  
138 depression required to yield the observed CCN activity. The long equilibration time  
139 (minutes or more) associated with adsorption (e.g., Schuttlefield et al., 2007) may explain  
140 why the hygroscopicity of dry and wet generated dust are so different. The residence time  
141 of dust particles in the instrumentation is typically less than a minute, limiting the amount  
142 of water that can adsorb and bias the observed hygroscopicity below its equilibrium  
143 value. Wetting the dust particles prior to measurement would maximize the amount of  
144 adsorbed water and express the full extent of its hygroscopicity. One approach to  
145 modeling this system is using one value for  $A_{FHH}$ ,  $B_{FHH}$ , combined with a variable uptake  
146 coefficient (that is very low during formation of the monolayer, and progressively  
147 increases with the number of adsorbed layers). Another explanation is the swelling of  
148 clays; during complete wetting, more surface area could be exposed for interaction,  
149 which would enhance dust hygroscopicity compared to a dry particle. Future work should  
150 focus on the existence and mechanism of adsorption/desorption transients.

#### 151 **4. Reconciling Dust Hygroscopicity under Subsaturated and Supersaturated** 152 **Conditions.**

153 Herich et al. (2009) measured water uptake on mineral dusts and different clays  
154 under subsaturated (with a hygroscopicity tandem differential mobility analyzer;  
155 HTDMA) and supersaturated (with a cloud condensation nuclei counter; CCNc)  
156 conditions. The hygroscopic growth factors (GF) were measured with a HTDMA, and the

157 CCN activity was measured using a CCNc. A poor correlation in experiments (deviation  
158 larger than  $\pm 50\%$ ) was found between  $\kappa$  derived from the HTDMA and CCNc. Herich et  
159 al. (2009) attributed this to resolution limitations in the HTDMA GF. Alternatively, KT  
160 may not adequately represent dust-water interactions, so that a single value of  $\kappa$  is not  
161 expected to describe the subsaturated water uptake and CCN activity for mineral dust  
162 aerosol. If FHH is more appropriate, then one set of  $A_{FHH}$  and  $B_{FHH}$  (neglecting the  
163 potential non-equilibrium artifacts) should reproduce both subsaturated and  
164 supersaturated properties of mineral dust aerosol, and is attempted below.

165 Gustafsson et al. (2005) studied the subsaturated hygroscopic uptake of ATD  
166 particles generated from suspensions in distilled water. Surface coverages as a function of  
167 RH were measured using a thermogravimetric analysis, during which multilayer  
168 adsorption (the number of water molecule layers,  $\theta \sim 3 - 4$ ) were observed for RH greater  
169 than 50%. Under such conditions, the FHH adsorption isotherm is applicable and is fitted  
170 to the data. The optimal values for  $A_{FHH}$  and  $B_{FHH}$  are 1.16 and 0.88, respectively, versus  
171 0.85 and 0.88 from CCN activation experiments (Table 1). Vlasenko et al. (2005)  
172 measured subsaturated hygroscopic growth of dry ATD; fitting a FHH adsorption  
173 isotherm to the growth data for  $RH > 70\%$  gives  $A_{FHH} = 0.19$  and  $B_{FHH} = 0.98$  (RMSE =  
174 0.035), which are very close to the FHH parameters obtained from CCN activation  
175 experiments for the same compound ( $A_{FHH} = 0.27$  and  $B_{FHH} = 0.79$ ; Table 1). Fitting FHH  
176 isotherms to the Gustafsson et al. (2005) and Hatch et al. (2008) measurements for  
177  $\text{CaCO}_3$  (different type from Table 1) gives  $A_{FHH} = 0.83-1.00$  and  $B_{FHH} = 0.76$ . All the  
178 above suggests that the adsorption parameters for similar samples are indeed consistent  
179 across different studies.

## 180 **5. Impact of KT and AT on CCN and Droplet Number**

181 In this section, differences in predicted CCN concentrations and droplet number  
182 concentrations from application of KT and FHH-AT are estimated. For this, we use a  
183 single-mode lognormal aerosol obtained from in-situ measurements of SD during the  
184 NAMMA field campaign (Twohy et al., 2009) (with geometric mean diameter,  $D_g = 0.10$   
185  $\mu\text{m}$ , standard deviation,  $\sigma_g = 1.6$ , and total particle concentration,  $N_\theta = 225$  per  $\text{cm}^3$ ). The  
186 CCN spectra computed with KT and FHH-AT (using  $\kappa$ ,  $A_{FHH}$ , and  $B_{FHH}$  listed in Table 1  
187 and the lognormal CCN spectra formulations of Kumar et al., 2009) are presented in  
188 Figure 2a. For supersaturations between 0.05% and 0.5% (a range relevant for cumulus  
189 and stratocumulus clouds), application of KT results in 8-12 times larger CCN than when  
190 applying FHH-AT. This is a direct consequence of  $x_\kappa < x_{FHH}$ , which tends to yield a larger  
191 activation fraction for KT-derived CCN spectra. For supersaturations greater than 0.5%,  
192 most aerosol in both distributions activate, so CCN computed by KT and FHH-AT  
193 converge.

194 The larger CCN concentrations (at a given supersaturation) associated with use of  
195 KT suggests that the calculated droplet number, compared to using FHH-AT, will be  
196 larger. KT however requires more water to activate particles than FHH-AT (Kumar et al.,  
197 2009), so the competition for water vapor in the former particles is stronger, potentially  
198 impacting  $s_{max}$  and  $N_d$ . For example for  $s_c = 0.05\%$ , the ratio of water volume at  $D_c$  in KT  
199 against FHH-AT ranges from 4.83 (dry ATD) to 15.43 (wet ATD). Hence for the same  
200 size distribution, the droplet number difference from application of each theory depends  
201 on two competing factors: *i*) the stronger competition of KT CCN for water vapor, and *ii*)  
202 the typically larger activation fraction associated with KT. These factors are

203 comprehensively accounted for in droplet number calculations carried out with the  
 204 Kumar et al. (2009) parameterization. In all droplet number calculations presented, the  
 205 parcel is assumed adiabatic, with initial temperature, 273 K; pressure, 600 mbar; and  
 206 updraft velocity,  $w$  ranging from  $0.1 \text{ ms}^{-1}$  to  $10 \text{ ms}^{-1}$ . For each dust type, the respective  $\kappa$   
 207 and FHH parameters ( $A_{FHH}$  and  $B_{FHH}$ ) from Table 1 are used.

208 Figure 2b shows the ratio of total CCN that activate to cloud droplets using KT,  $N_d^\kappa$ ,  
 209 to that from FHH-AT,  $N_d^{FHH}$ , as a function of parcel updraft velocity (symbols) for four  
 210 different dust types. The corresponding parcel  $s_{max}$  is also shown (solid lines). For wet  
 211 CID and wet ATD,  $\frac{N_d^\kappa}{N_d^{FHH}}$  is largest ( $\sim 1.3 - 1.4$ ) at  $w \sim 0.1 \text{ ms}^{-1}$  and approaches 1.0 for  $w$   
 212  $> 1 \text{ ms}^{-1}$ . This is because the parcel  $s_{max} < 1\%$  for all  $w < 1 \text{ ms}^{-1}$  (Figure 2b), where  
 213  $\frac{F_k}{F_{FHH}} > 1$  (Figure 2a) and droplet differences are dominated by the larger activation  
 214 fractions associated with KT. Similarly,  $\frac{F_k}{F_{FHH}} > 1$  for dry ATD and SD and  $w < 1 \text{ ms}^{-1}$ .  
 215 However, for  $w > 1 \text{ ms}^{-1}$ , the competition of water vapor from KT particles is sufficiently  
 216 strong so that  $\frac{N_d^\kappa}{N_d^{FHH}} < 1$ . At very high updrafts ( $> 3 \text{ ms}^{-1}$ ), all particles activate,  
 217 and  $\frac{N_d^\kappa}{N_d^{FHH}} \rightarrow 1$ .

## 218 6. Conclusions.

219 In this study, we compared Köhler theory (KT) against FHH adsorption activation  
 220 theory (FHH-AT) when applied to the activation of mineral dust aerosol. Based on

221 published data, a number of potential issues were found with KT, suggesting it may not  
222 fully represent CCN activity of mineral dust aerosol, since *i*) a consistent set of FHH-AT  
223 adsorption parameters can be found that describe both the subsaturated hygroscopic  
224 growth and CCN activity, and, *ii*) the critical supersaturation vs dry diameter exponents  
225 determined for FHH-AT are often closer to observations, than those from KT.  
226 Application of KT and FHH-AT leads to the differences in predicted CCN and cloud  
227 droplet number concentrations, even if consistent hygroscopicity and adsorption  
228 parameters (i.e., derived from the same experimental data) are used. For the dust samples  
229 considered here, CCN concentrations can differ by a factor of 10, and results in a 40%  
230 difference in predicted cloud droplet number concentration. Thus, a comprehensive  
231 description of CCN activity of mineral dust aerosol throughout its atmospheric lifetime  
232 may require a combination of both KT and FHH-AT.

### 233 **Acknowledgements**

234 This work was supported by the NOAA ACC Program. AN acknowledges support from  
235 NSF CAREER and NASA-ACMAP grants.

### 236 **References**

- 237 Crittenden, B. D., and W. J. Thomas (1998), Adsorption technology and design,  
238 Butterworth-Heinemann, ISBN 0750619597.
- 239 DeMott, P. J., K. Sassen, M. R. Poellot, D. Baumgardner, D. C. Rogers, S. D. Brooks, A.  
240 J. Prenni, and S. M. Kreidenweis (2003), African dust aerosols as atmospheric ice  
241 nuclei, *Geophys. Res. Lett.*, 30(14), 1732, doi:10.1029/2003GL017410.

242 Field, P. R., O. Möhler, P. Connolly, M. Krämer, R. Cotton, A. J. Heymsfield, H.  
243 Saathoff, and M. Schnaiter (2006), Some ice nucleation characteristics of Asian and  
244 Saharan desert dust, *Atmos. Chem. Phys.*, 6, 2991-3006.

245 Fountoukis, C., and A. Nenes (2007), ISORROPIA II: a computationally efficient aerosol  
246 thermodynamic equilibrium model for  $K^+$ ,  $Ca^{2+}$ ,  $Mg^{2+}$ ,  $NH_4^+$ ,  $Na^+$ ,  $SO_4^{2-}$ ,  $NO_3^-$ ,  $Cl^-$ ,  
247  $H_2O$  aerosols, *Atmos. Chem. Phys.*, 7, 4639-4659.

248 Gustafsson, R. J., A. Orlov, C. L. Badger, P. T. Griffiths, R. A. Cox, and R. M. Lambert  
249 (2005), A comprehensive evaluation of water uptake on atmospherically relevant  
250 mineral surfaces: DRIFT spectroscopy, thermogravimetric analysis and aerosol  
251 growth measurements, *Atmos. Chem. Phys.*, 5, 3415–3421.

252 Hatch, C. D., K. M. Gierlus, J. D. Schuttlefield, and V. H. Grassian (2008), Water  
253 adsorption and cloud condensation nuclei activity of calcite and calcite coated with  
254 model humic and fulvic acids, *Atmos. Environ.*, 42, 5672-5684.

255 Herich, H., T. Tritscher., A. Wiacek, M. Gysel, E. Weingartner, U. Lohmann, U.  
256 Baltensperger, and D. J. Cziczo (2009), Water uptake of clay and desert dust  
257 aerosol particles at sub- and supersaturated water vapor conditions, *Phys. Chem.*  
258 *Chem. Phys.*, doi:10.1039/b901585j.

259 Henson, B. F. (2007), An adsorption model of insoluble particle activation: Application  
260 to black carbon, *J. Geophys. Res.*, 112, D24S16, doi:10.1029/2007JD008549.

261 Koehler, K. A. (2008), The impact of natural dust aerosol on warm and cold cloud  
262 formation, Ph.D. dissertation thesis, 208 pp., Colo. State Univ., Fort Collins.

263 Koehler, K. A., S. M. Kreidenweis, P. J. DeMott, M. D. Petters, A. J. Prenni, and C. M.  
264 Carrico (2009), Hygroscopicity and cloud droplet activation of mineral dust aerosol,  
265 *Geophys. Res. Lett.*, *36*, L08805, doi:10.1029/2009GL037348.

266 Köhler, H. (1936), The nucleus in and the growth of hygroscopic droplets, *Trans. Faraday*  
267 *Soc.*, *32*(2), 1152-1161.

268 Kumar, P., I. N. Sokolik, and A. Nenes (2009), Parameterization of cloud droplet  
269 formation for global and regional models: including adsorption activation from  
270 insoluble CCN, *Atmos. Chem. Phys.*, *9*, 2517-2532.

271 Levin, Z., and W. R. Cotton (2007), Aerosol pollution impact on precipitation: A  
272 scientific review, WMO/IUGG Report.

273 Nenes., A., S. Ghan, H. Abdul-Razzak, P. Y. Chuang, and J. H. Seinfeld (2001), Kinetic  
274 Limitations on Cloud Droplet Formation and Impact on Cloud Albedo, *Tellus*, *53B*,  
275 133-149.

276 Petters, M. D., and S. M. Kreidenweis (2007), A single parameter representation of  
277 hygroscopic growth and cloud condensation nucleus activity, *Atmos. Chem. Phys.*,  
278 *7*, 1961-1971.

279 Rosenfeld, D., Y. Rudich, and R. Lahav (2001), Desert dust suppressing precipitation: A  
280 possible desertification feedback loop, *Proc. Natl. Acad. Sci. U.S.A.*, *98*(11), 5975-  
281 5980.

282 Schuttlefield, J. D., D. Cox, and V. H. Grassian (2007), An investigation of water uptake  
283 on clays minerals using ATR-FTIR spectroscopy coupled with quartz crystal  
284 microbalance measurements, *J. Geophys. Res.*, *112*, D21303,  
285 doi:10.1029/2007JD008973.

286 Sorjamaa, R. and A. Laaksonen (2007), The effect of H<sub>2</sub>O adsorption on cloud drop  
287 activation of insoluble particles: a theoretical framework, *Atmos. Chem. Phys.*, 7,  
288 6175-6180.

289 Sullivan, R. C., M. J. K. Moore, M. D. Petters, S. M. Kreidenweis, G. C. Roberts, and K.  
290 A. Prather (2009), Effect of chemical mixing state on the hygroscopicity and cloud  
291 nucleation properties of calcium mineral dust particles, *Atmos. Chem. Phys.*, 9,  
292 3303-3316.

293 Twohy, C. H., S. M. Kreidenweis, T. Eidhammer, E. V. Browell, A. J. Heymsfield, A.  
294 R. Bansemer, B. E. Anderson, G. Chen, S. Ismail, P. J. DeMott, and S. C. Van Den  
295 Heever (2009), Saharan dust particles nucleate droplets in eastern Atlantic clouds,  
296 *Geophys. Res. Lett.*, 36, L01807, doi:10.1029/2008GL035846.

297 Vlasenko, A., S. Sjögren, E. Weingartner, H. W. Gäggeler, and M. Ammann (2005),  
298 Generation of Submicron Arizona Test Dust Aerosol: Chemical and Hygroscopic  
299 Properties, *Aer. Sci. Tech.*, 39 (5), 452-460.

300 **Table 1:** FHH parameters for different mineral dusts and dust related compounds  
 301 composites. FHH adsorption activation fits to the experimental CCN activity data  
 302 obtained from Koehler et al. (2009) and Sullivan et al. (2009).

Description (Acronym)	Generation*	$\kappa$	$A_{FHH}$	$B_{FHH}$	$x_{\kappa}$	$x_{FHH}$	$x_{exp}$
Arizona Test Dust (ATD)	Dry	0.025	0.27	0.79	-1.43	-1.20	-1.39
Arizona Test Dust (ATD)	Wet	0.35	0.85	0.88	-1.49	-1.26	-1.36
Owens Lake (OL)	Wet	0.39-1.07	1.14	0.91	-1.50	-1.25	-1.36
Canary Island Dust (CID)	Wet	0.26	0.80	0.88	-1.49	-1.24	-1.33
Saharan Dust (SD)	Dry	0.054	0.42	0.83	-1.47	-1.23	-1.42
Calcium Nitrate (Ca(NO <sub>3</sub> ) <sub>2</sub> )	Wet	0.51	1.13	0.90	-1.50	-1.30	-1.59
Oxalic Acid (C <sub>2</sub> O <sub>4</sub> H <sub>2</sub> )	Wet	0.50	1.02	0.90	-1.50	-1.27	-1.35
Calcium Carbonate (CaCO <sub>3</sub> )	Dry	0.0011	0.25	1.19	-1.18	-0.96	-0.96
Calcium Sulfate (CaSO <sub>4</sub> )	Dry	0.0016	0.10	0.91	-1.21	-1.02	-1.02
Calcium Oxalate Monohydrate (COH or CaC <sub>2</sub> O <sub>4</sub> .H <sub>2</sub> O)	Dry	0.048	0.57	0.88	-1.47	-1.15	-1.16

303 \*"Dry" refers to dust particles generated with a fluidized bed; "Wet" refers to atomization from an  
 304 aqueous solution/suspension

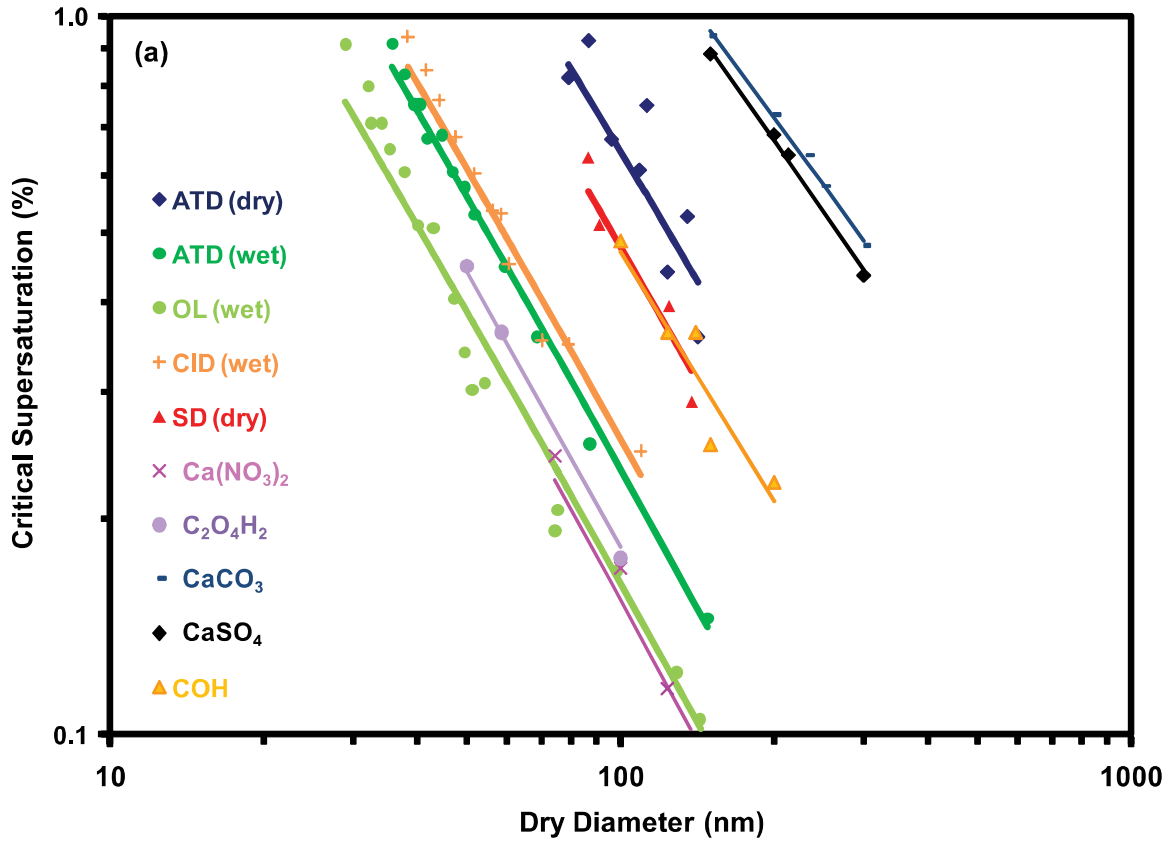
305 **Figure Captions**

306 **Figure 1. (a):** FHH adsorption activation fits (lines) to the observed CCN activity  
307 (points) for dust types presented in Table 1. Data obtained from Figure 7.1 (pp 154) and  
308 Figure 5 from Koehler et al. (2009) and Sullivan et al. (2009), respectively. “Dry” refers  
309 to dust particles generated with a fluidized bed, and “wet” refers to atomization from an  
310 aqueous suspension. **(b):** Comparison between  $x_{exp}$ ,  $x_{\kappa}$  (circles) and  $x_{FHH}$  (squares). Color  
311 scheme identical to (a). Dashed lines represent  $\pm 7.5\%$  deviation from 1:1 line.

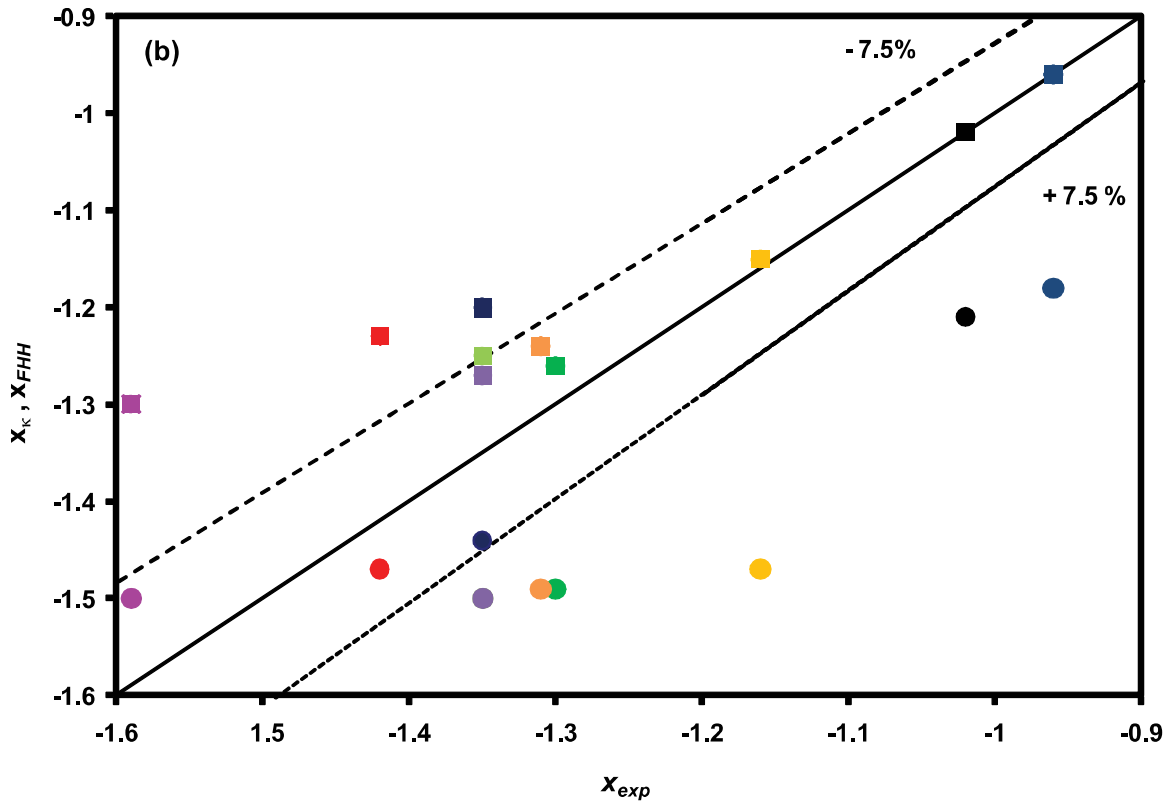
312

313 **Figure 2: (a):** Ratio of CCN spectrum given by Köhler theory to that given by FHH  
314 adsorption activation theory as a function of supersaturation. Numbers noted on each  
315 curve refer to the ratio of water volume required by KT over FHH-AT to activate a CCN  
316 with  $s_c = 0.05\%$ . **(b):** Ratio of parameterized activated fraction (points) for different dust  
317 types as a function of increasing updraft velocity in a cloud parcel. Also shown are the  
318 corresponding parcel  $s_{max}$  (lines) for each dust type. Color scheme identical to (a). Dust  
319 types defined in Table 1.

320

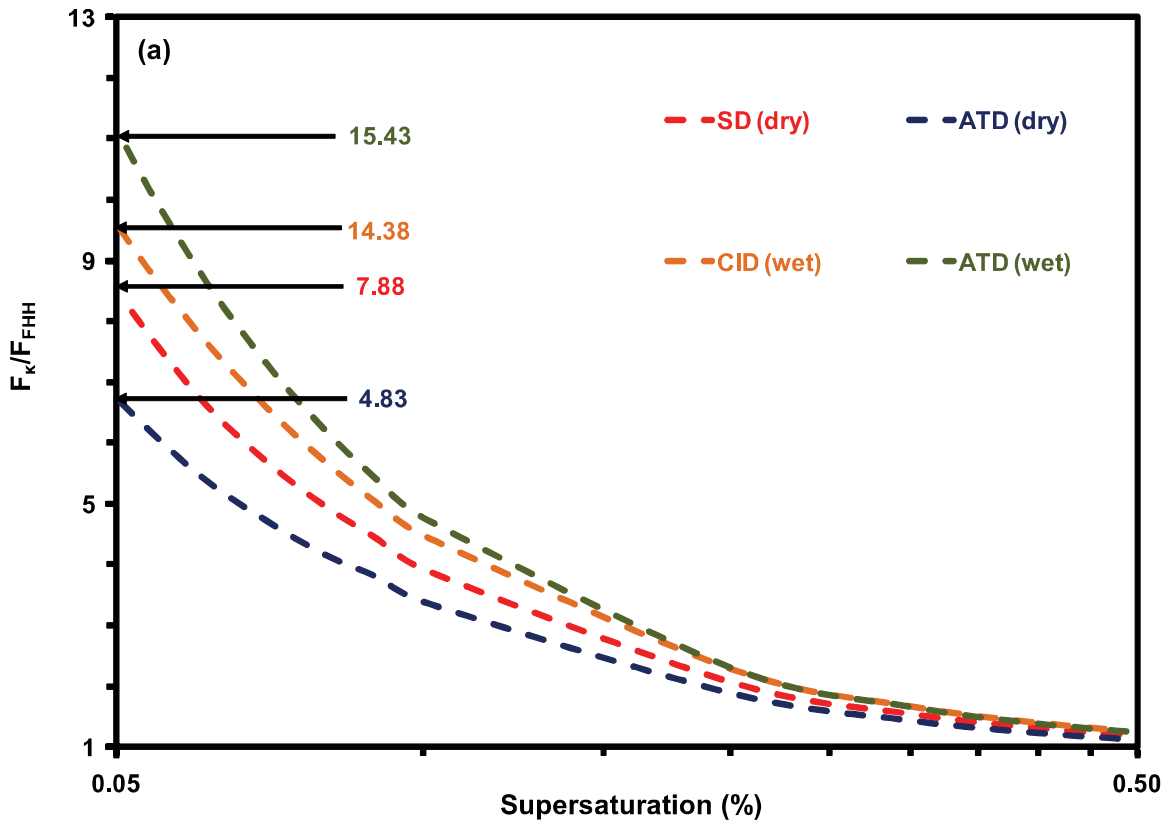


321  
322

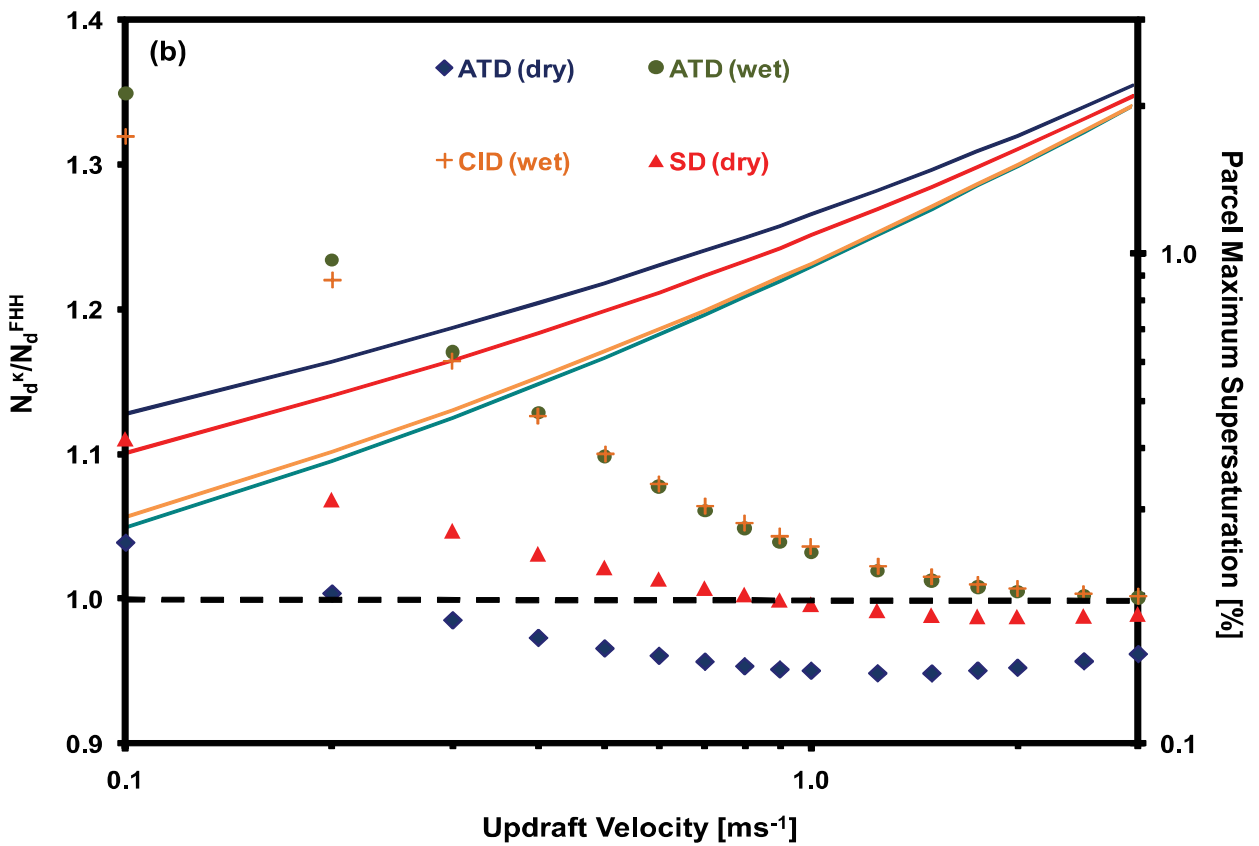


323  
324

Figure 1



325  
326



327  
328

Figure 2